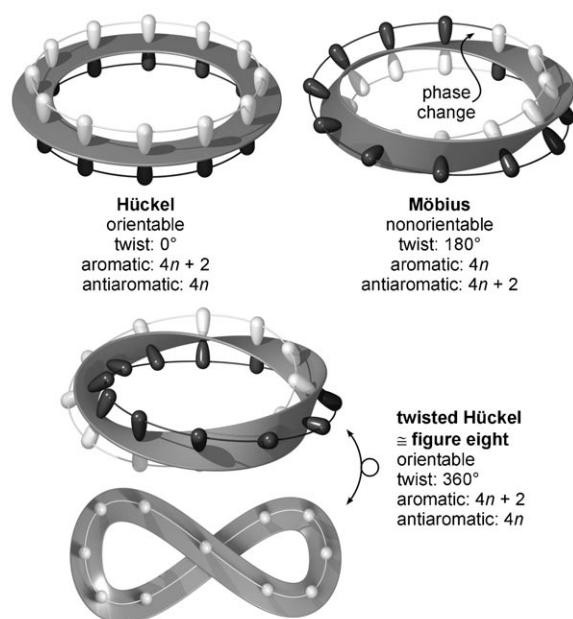


# Expanded Porphyrin with a Split Personality: A Hückel–Möbius Aromaticity Switch\*\*

Marcin Stępień, Lechosław Latos-Grażyński,\* Natasza Sprutta, Paulina Chwalisz, and Ludmiła Szterenber

Möbius aromaticity<sup>[1,2]</sup> is an intriguing and rarely encountered type of electron delocalization, so called because of its formal relationship to the famous Möbius band, the classical example of a one-sided (nonorientable) surface. Möbius  $\pi$  systems (Scheme 1) are characterized by a 180° twist, which signifi-



**Scheme 1.** Topologies of conjugated  $\pi$ -electron systems with different numbers of half twists; the number of  $\pi$  electrons in the aromatic and antiaromatic systems is given in each case.

cantly affects their electronic structure. In particular, the Hückel rule, observed by untwisted annulenes, is reversed, and  $4n$ -electron Möbius annulenes are aromatic (stabilized)

whereas the  $(4n+2)$ -electron systems are antiaromatic (destabilized).<sup>[1–3]</sup> In more general terms, conjugated cyclic molecules can be classified as Hückel or Möbius systems, depending on the number of half twists in the ring (even or odd, respectively). The molecules with an even number of half twists are predicted to follow the Hückel rule, whereas those with an odd number of half twists (Möbius systems) follow the reverse Hückel rule.<sup>[2]</sup> Scheme 1 shows the “twisted Hückel” topology, characterized by two half twists, which is equivalent to the figure-eight structure found in certain aromatic systems.<sup>[4]</sup>

Even though Möbius aromaticity was first considered over 40 years ago,<sup>[3]</sup> it is still more easily demonstrated *in silico* than *in vitro*. While Möbius-type structures were proposed as transition states<sup>[5–8]</sup> and reactive intermediates,<sup>[9]</sup> the first examples of stable, neutral Möbius  $\pi$  systems have been synthesized only recently.<sup>[10,11]</sup> In those carefully designed molecules, developed by Herges and co-workers, the twist was achieved by combining normal and in-plane conjugation. The resultant rigid framework helped prevent isomerization between Hückel and Möbius topologies. On the other hand, flexible systems, such as the higher annulenes, preferentially adopt untwisted (Hückel) topologies, which are normally less strained.<sup>[1,2,12]</sup> While computational data indicate that Möbius conformations might contribute to the chemistry of higher  $[4n]$ annulenes,<sup>[12]</sup> so far they have not been identified experimentally. Herein we show the first example of dynamic switching between Hückel and Möbius topologies in a conjugated molecule. This effect is observed in an expanded porphyrin analogue containing *para*-phenylene rings. When incorporated into a macrocyclic structure, *p*-phenylene units are known to enable partial conjugation while retaining their rotational freedom.<sup>[13,14]</sup>

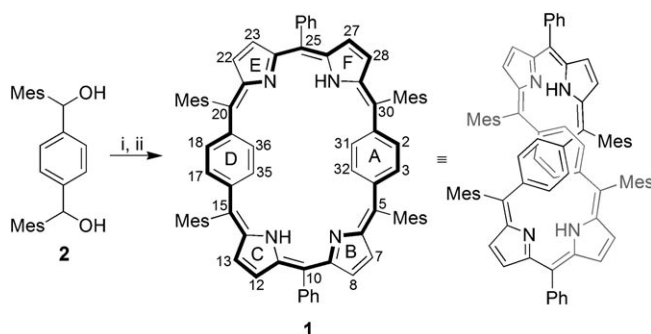
The compound A,D-di-*p*-benzi[28]hexaphyrin(1.1.1.1.1.1) (**1**; A and D denote the positions of the phenylene rings in the macrocyclic structure) was obtained in an acid-catalyzed condensation of dicarbinol **2** with pyrrole and benzaldehyde, and subsequent oxidation with DDQ (Scheme 2). The resulting molecule bears four mesityl and two phenyl substituents. The bulk of the mesityl groups assists the formation of expanded macrocycles and additionally prevents molecular aggregation. Structurally, this new system combines the features of expanded porphyrins<sup>[15,16]</sup> and benziporphyrins, the phenylene-containing porphyrinoids.<sup>[13,17]</sup> The oxidation level of this system corresponds to a 28- $\pi$ -electron conjugation pathway (Scheme 2).

The molecular structure of **1**, obtained from X-ray structural analysis, is shown in Figure 1. Compound **1** has crystallographic  $C_2$  symmetry and, like many other expanded

[\*] Dr. M. Stępień, Prof. L. Latos-Grażyński, Dr. N. Sprutta, P. Chwalisz, Dr. L. Szterenber  
Wydział Chemii  
Uniwersytet Wrocławski  
ul F. Joliot-Curie 14, 50-383 Wrocław (Poland)  
Fax: (+48) 71-328-2348  
E-mail: llg@wchuwr.pl

[\*\*] Financial support from the Ministry of Science and Higher Education (Grant PBZ-KBN-118/T09/2004) is kindly acknowledged. DFT calculations were carried out at the Supercomputer Centers of Poznań and Wrocław. We thank Prof. Tadeusz Lis for experimental assistance.

Supporting information for this article is available on the WWW under <http://www.angewandte.org> or from the author.



**Scheme 2.** Synthesis of di-*p*-benzihexaphyrin. Reagents and conditions: i) pyrrole (2 equiv), benzaldehyde (1 equiv),  $\text{CH}_2\text{Cl}_2$ , cat.  $\text{BF}_3 \cdot \text{Et}_2\text{O}$ ; ii) 2,3-dichloro-5,6-dicyano-1,4-benzoquinone (DDQ, 2 equiv). The 28- $\pi$ -electron pathway is shown in bold.

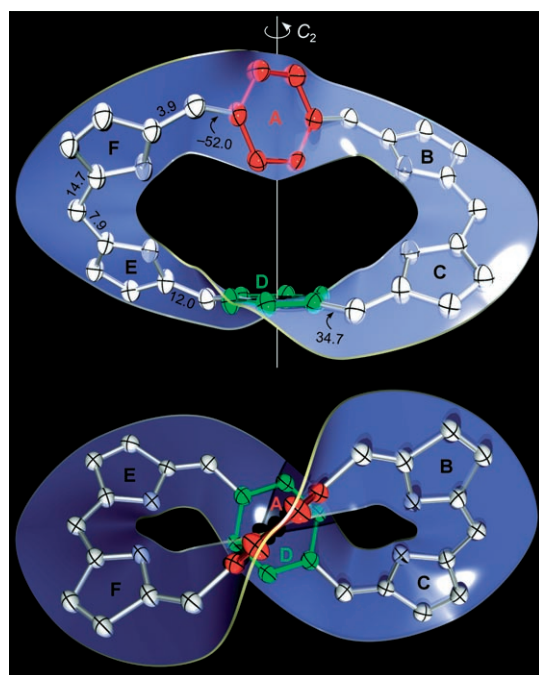


**Figure 1.** X-ray crystal structure of **1** with thermal ellipsoids at the 50% probability level.<sup>[28]</sup> Meso substituents, hydrogen atoms, and solvent molecules are omitted for clarity. The two nonequivalent phenylene rings are shown in red and green, and nitrogen atoms are highlighted in blue. The elastic band follows the surface of the  $\pi$  system. Dihedral angles at the  $\text{C}_{\text{meso}}\text{--C}_\alpha$  bonds are given in degrees. An animated version of this figure is available in the Supporting Information.

porphyrins,<sup>[18–24]</sup> adopts a figure-eight conformation, with the two phenylene rings located at the intersection. However, these two rings, denoted A and D in Figure 1, are not equivalent, being respectively parallel and perpendicular to the symmetry axis, and they are aligned in an “edge-to-face” fashion. The distance of the inner hydrogen atoms of ring A to the mean plane of ring D is 2.98 Å. Because of the non-planarity of **1**, its  $\pi$  system is torsionally distorted, with the largest dihedral angle (52°) adjacent to ring A. As a consequence of the unusual arrangement of the phenylene rings, the surface of the  $\pi$  system is single-sided, and corresponds to the Möbius band with a single half twist. To the best of our

knowledge, **1** is the first example of this topology recognized among expanded porphyrins and *para*-cyclophane derivatives. As with other figure-eight expanded porphyrins, **1** is intrinsically chiral but crystallizes in a racemic space group (*Pccn*).

The Möbius conformation of **1**, observed in the crystal structure, is not rigid, and the nonequivalence of the phenylene rings is lost in solution, as evidenced by  $^1\text{H}$  NMR spectroscopy. The spectrum of **1**, recorded in  $[\text{D}]\text{chloroform}$  at 293 K, contains only one phenylene signal (Figure 2).

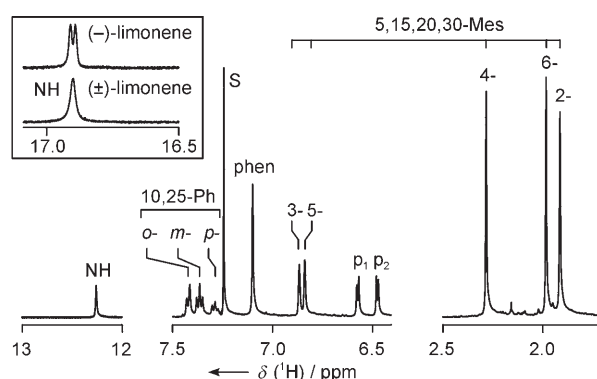


**Figure 2.**  $^1\text{H}$  NMR spectrum of **1** ( $\text{CDCl}_3$ , 293 K). Numbering follows that given in Scheme 2. Labels: phen = 2,3,17,18,31,32,35,36-H,  $p_1$  = 8,12,23,27-H,  $p_2$  = 7,13,22,28-H, S = solvent. Peaks were assigned on the basis of 2D correlation spectra. Inset shows the NH signal of **1** dissolved in optically active (–)-limonene and racemic (±)-limonene.

Except for that signal (see below), the observed spectrum is consistent with a  $D_2$  symmetry of the molecular framework. This symmetry is higher than expected for any conceivable instantaneous configuration of **1**, and provides important information about the nature and timescale of dynamic processes affecting the molecule:

1. The NH protons are rapidly scrambled among all nitrogen atoms. This process, which probably occurs independently in each dipyrromethene subunit, is very fast and similar to intramolecular proton transfer observed in porphyrins.<sup>[25]</sup>
2. Both phenylene rings are equivalent on the NMR timescale and rotate freely, leading to coalescence of the phenylene signals (two resonances are expected for a rigid  $D_2$ -symmetric structure). Similar behavior was previously observed in *p*-benziporphyrin, a smaller congener of **1**.<sup>[13]</sup>
3. The macrocycle is otherwise rigid and its figure-eight twist does not unfold into a planar or boatlike conformation, or this process is very slow on the NMR timescale. This rigidity is likely induced by the steric bulk of the four mesityl substituents. Consequently, no exchange (racemization) occurs between the enantiomers of **1**. Such a dynamic process would result in a higher effective symmetry ( $D_{2h}$ ) and in the averaging of the *ortho*-methyl signals of the mesityl substituents (labeled 2- and 6- in Figure 2). Similar rigidity of the figure-eight twist was observed in the octaphyrins reported by Vogel et al.,<sup>[19]</sup> which were actually separated into enantiomers.<sup>[21]</sup> In this

work, the absence of racemization was additionally confirmed by recording the  $^1\text{H}$  NMR spectrum of **1** in (–)-limonene. In this experiment, the use of a chiral solvent enabled the observation of a separate NH peak for each enantiomer (Figure 2, inset).

The symmetry of the spectrum in  $\text{CDCl}_3$  is unchanged over a range of temperatures (203–343 K, Figure S1 in the Supporting Information). This observation indicates that both the NH tautomerization and phenylene rotation are in the fast-exchange limit, even at 203 K. However, as the temperature is varied, the chemical shifts of all signals experience remarkable changes of varying direction and magnitude (Figure 3, and Figure S1 in the Supporting Information). This effect can be explained by assuming a temperature-dependent equilibrium between two species, denoted **1-H** and **1-M**, the latter prevailing at lower temperatures. The chemical shift data were fitted numerically to the van't Hoff equation, and the assumed model was found to be very accurate (Figure 3, see also the Supporting Information). The equilibrium constant  $K = [\text{1-H}]/[\text{1-M}]$  varies from  $1.41 \times 10^{-2}$  at 203 K to 1.43 at 343 K. The temperature dependence of  $K$  provides the thermodynamic parameters for the equilibrium:  $\Delta H = 19.1(4) \text{ kJ mol}^{-1}$  and  $\Delta S = 58.7(1.1) \text{ J mol}^{-1} \text{ K}^{-1}$ .

In addition to the thermodynamic data, the extrapolated chemical shifts of pure **1-H** and **1-M** were also determined (Table 1). Examination of these values reveals that a significant paratropic ring current is present in **1-H**. The other species, **1-M**, displays chemical shifts characteristic of porphyrinoids devoid of macrocyclic aromaticity.<sup>[17]</sup> The paratropicity of **1-H** is especially evident from the chemical shifts in the dipyrromethane fragments. In particular, the NH signal experiences a strong downfield shift to  $\delta = 16.51 \text{ ppm}$ ,

**Table 1:**  $^1\text{H}$  NMR chemical shifts of conformers **1-H** and **1-M**.

Signal <sup>[a]</sup>	$\delta(\text{1-H})$ [ppm]			$\delta(\text{1-M})$ [ppm]	
	$\text{C}_6\text{D}_{14}$	$\text{CDCl}_3$ <sup>[b]</sup>	GIAO <sup>[c]</sup>	$\text{CDCl}_3$ <sup>[b]</sup>	GIAO <sup>[c]</sup>
NH	16.30	16.51	19.12	10.31	6.97
phen	8.03	8.18	9.43	6.60	5.87
<i>o</i> - (Ph)	7.14	7.15	6.75	7.55	7.90
<i>m</i> - (Ph)	7.17	7.21	7.09	7.43	7.60
<i>p</i> - (Ph)	7.09	7.17	7.06	7.34	7.49
3- (Mes)	7.08	7.16	7.55	6.68	6.63
5- (Mes)	6.72	6.75	6.83	6.93	7.12
$p_1$	6.22	6.16	5.80	6.76	7.06
$p_2$	6.08	6.10	5.81	6.64	6.96
4- (Mes)	2.32	2.38	2.36	2.23	2.14
2- (Mes)	2.81	2.97	4.03	1.42	0.65
6- (Mes)	1.45	1.40	0.83	2.25	2.68

[a] Labeling follows that in Figure 2. [b] Extrapolated. [c] Calculated chemical shifts (GIAO-B3LYP/6-31G\*\*<sup>+</sup>; B3LYP/6-31G\*\* geometries) averaged according to the assumed model of exchange.

whereas signals  $p_1$ ,  $p_2$ , and *o*-Ph are shifted upfield relative to their positions in **1-M**.

According to the Hückel rule, the 28- $\pi$ -electron system of **1** (Scheme 2) should display paratropicity, provided that the macrocycle adopts a Hückel-type topology (either twisted or planar). Even though defining ring currents in figure-eight loops is far from straightforward,<sup>[2]</sup> both dia- and paratropic effects were previously observed in figure-eight cyclophanes<sup>[4]</sup> and expanded porphyrins.<sup>[23]</sup> Thus, in accordance with the aromaticity rules described in the introduction,<sup>[1–3]</sup> the paratropic species **1-H** corresponds to the Hückel topology, whereas **1-M** is the Möbius system. In principle, **1-M** should be diatropic, but the ring current is not observed, likely because of torsional strain, which results in inefficient overlap of the p orbitals.<sup>[2]</sup>

Subsequently it was discovered that the equilibrium between **1-H** and **1-M** is solvent-dependent. In some solvents, such as aliphatic hydrocarbons and alcohols, only **1-H** is observed. The  $^1\text{H}$  NMR chemical shifts measured in  $[\text{D}_{14}]\text{hexane}$  for **1** are in extraordinary agreement with the extrapolated values for **1-H** obtained in  $[\text{D}]\text{chloroform}$ . On the other hand, in solvents such as benzene or dichloromethane, a certain amount of **1-M** is also present and it becomes the dominant conformer in chloroform and *N,N*-dimethylformamide. Even though the two species should have different dipole moments (it is expected to be 0 for **1-H**), there is no simple relationship between the equilibrium constant and solvent polarity. Apparently, specific interactions with the phenylene rings of **1** contribute to the observed solvent effects.

The dependence of the proposed equilibrium on both temperature and solvent was further investigated by using electronic spectroscopy. Here, advantage was taken of the different timescale of this method, thereby enabling observation of separate absorption transitions for the exchanging species. As shown in Figure 4, the two forms **1-H** and **1-M** possess vastly different optical signatures. In accord with the NMR results, lowering the temperature of a chloroform

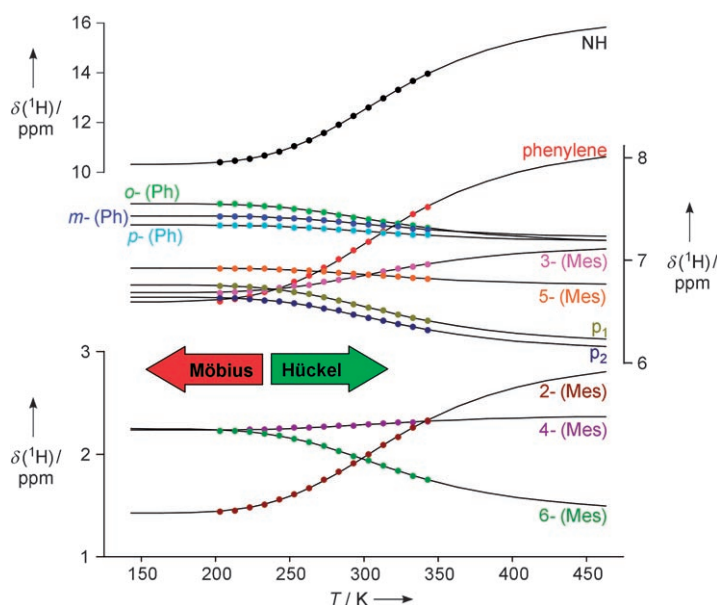


**Figure 3.**  $^1\text{H}$  NMR chemical shifts of **1** in  $\text{CDCl}_3$  plotted as a function of temperature. Experimental points are represented by filled circles. Solid curves correspond to chemical shifts calculated from the van't Hoff equation. Arrows indicate the increase in concentration of **1-H** (Hückel) and **1-M** (Möbius). Numerical details are given in the Supporting Information.



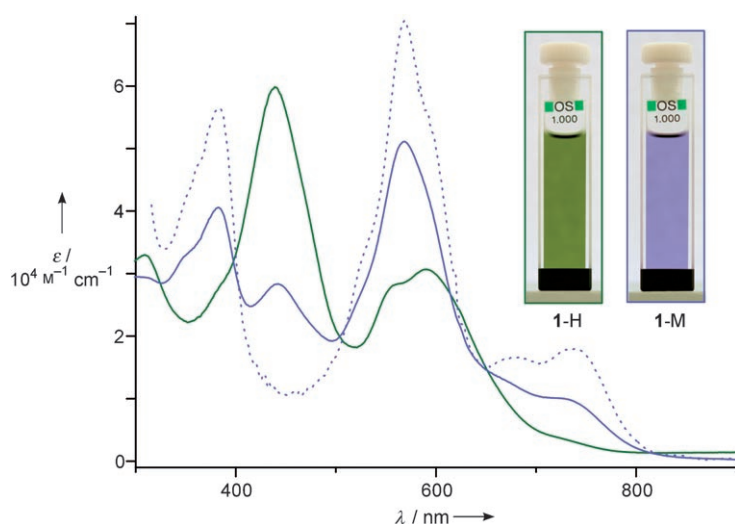


**Figure 4.** Electronic-absorption spectra of **1** recorded at 293 K in hexane (green, 100% **1-H**) and chloroform (blue, 68% **1-M**). The low-temperature spectrum ( $\text{CHCl}_3$ , ca. 210 K, 99% **1-M**) is shown as blue dots. The photographs were taken at room temperature.

solution results in an increase of the concentration of the Möbius conformer.

Further support for the proposed conformational exchange was obtained from DFT calculations. The geometries of **1-H** and **1-M** were optimized at the B3LYP/6-31G\*\* level of theory (Figure 5). In **1-H**, the phenylene rings are equivalent and coplanar, leading to a twisted Hückel topology, which is common to all figure-eight porphyrinoids (see Scheme 1). On the other hand, the edge-to-face arrangement, observed in the X-ray structure, is reproduced in the structure of **1-M**. In agreement with the experimental findings, the two conformers, **1-H** and **1-M**, are predicted to have comparable energies, the Hückel structure being more

stable by  $12.6 \text{ kJ mol}^{-1}$ . The exact energy ordering has no quantitative significance as the calculations were performed without a solvent model.

The  $^1\text{H}$  NMR chemical shifts calculated for the DFT geometries of **1-H** and **1-M** using the GIAO method are given in Table 1. There is a very good qualitative agreement between calculated and experimental shifts, even though the paratropicity of **1-H** (and, in fact, the diatropicity of **1-M**) is significantly exaggerated. This effect is likely due to the known propensity of the B3LYP functional to overestimate  $\pi$  conjugation.<sup>[26]</sup> Nevertheless, there is a remarkably good linear correlation between the calculated and experimental shift differences between **1-H** and **1-M** (see the Supporting Information).

This contribution describes the synthesis and properties of a dynamic Hückel–Möbius system, whose behavior was studied by using spectroscopic and computational methods. In this system, the *p*-phenylene ring is used for the first time as a “topology selector”. As shown in Figure 5, each of the two orientations of the phenylene ring induces a  $90^\circ$  helical twist that is either left- or right-handed.

Consequently, upon rotating the selector ring by  $90^\circ$ , the overall twist is reduced or increased by  $180^\circ$ , leading to a change in topology of the  $\pi$  system.<sup>[27]</sup> Compound **1** employs this effect to provide a topologically switchable chromophore, a feature that might be useful in the design of functional receptor systems. Phenylene-containing porphyrinoids hold particular promise in this regard, as they are capable both of metal coordination and anion binding. Efforts to explore these possibilities are underway.

Received: February 7, 2007

Published online: July 2, 2007

**Keywords:** aromaticity · conformation analysis · conjugation · NMR spectroscopy · porphyrinoids

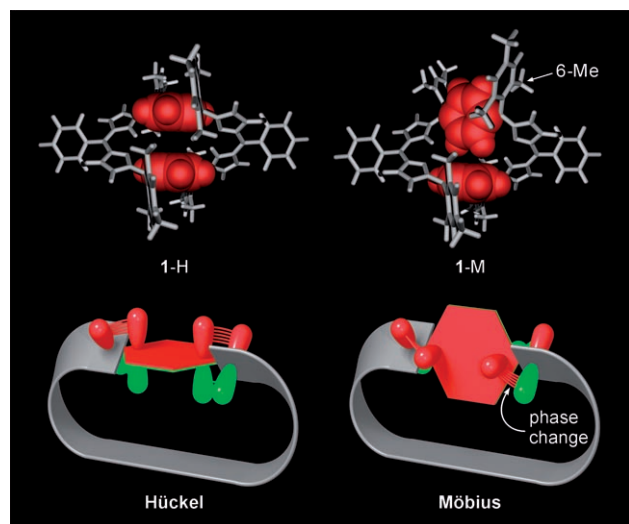


**Figure 5.** DFT-optimized geometries of **1-H** and **1-M** (top). The assignment of the mesityl 6-Me signal is based on the calculated chemical shifts. Bottom panels depict the action of the phenylene ring as a “topology selector”. The Hückel and Möbius conformers are characterized respectively by a left- and right-handed helical twist.

- [1] H. S. Rzepa, *Chem. Rev.* **2005**, *105*, 3697–3715.
- [2] R. Herges, *Chem. Rev.* **2006**, *106*, 4820–4842.
- [3] E. Heilbronner, *Tetrahedron Lett.* **1964**, *5*, 1923–1928.
- [4] H. Hinrichs, A. J. Boydston, P. G. Jones, K. Hess, R. Herges, M. M. Haley, H. Hopf, *Chem. Eur. J.* **2006**, *12*, 7103–7115.
- [5] H. E. Zimmerman, *J. Am. Chem. Soc.* **1966**, *88*, 1564–1565.
- [6] C. Castro, W. L. Karney, M. A. Valencia, C. M. H. Vu, R. P. Pemberton, *J. Am. Chem. Soc.* **2005**, *127*, 9704–9705.
- [7] J. F. Moll, R. P. Pemberton, M. G. Gutierrez, C. Castro, W. L. Karney, *J. Am. Chem. Soc.* **2007**, *129*, 274–275.
- [8] R. P. Pemberton, C. M. McShane, C. Castro, W. L. Karney, *J. Am. Chem. Soc.* **2006**, *128*, 16692–16700.
- [9] M. Mauksch, V. Gogonea, H. Jiao, P. von R. Schleyer, *Angew. Chem.* **1998**, *110*, 2515–2517; *Angew. Chem. Int. Ed.* **1998**, *37*, 2395–2398.
- [10] D. Ajami, O. Oeckler, A. Simon, R. Herges, *Nature* **2003**, *426*, 819–821.
- [11] D. Ajami, K. Hess, F. Köhler, C. Näther, O. Oeckler, A. Simon, C. Yamamoto, Y. Okamoto, R. Herges, *Chem. Eur. J.* **2006**, *12*, 5434–5445.
- [12] C. Castro, C. M. Isborn, W. L. Karney, M. Mauksch, P. von R. Schleyer, *Org. Lett.* **2002**, *4*, 3431–3434.

- [13] M. Stępień, L. Latos-Grażyński, *J. Am. Chem. Soc.* **2002**, *124*, 3838–3839.
- [14] K. Müllen, H. Unterberg, W. Huber, O. Wennerström, U. Norinder, D. Tanner, B. Thulin, *J. Am. Chem. Soc.* **1984**, *106*, 7514–7522.
- [15] J. L. Sessler, A. Gebauer, S. J. Weghorn in *The Porphyrin Handbook*, Vol. 2 (Eds.: K. M. Kadish, K. M. Smith, R. Guilard), Academic Press, San Diego, CA, **2000**, pp. 55–124.
- [16] J. L. Sessler, D. Seidel, *Angew. Chem.* **2003**, *115*, 5292–5333; *Angew. Chem. Int. Ed.* **2003**, *42*, 5134–5175, .
- [17] M. Stępień, L. Latos-Grażyński, *Acc. Chem. Res.* **2005**, *38*, 88–98.
- [18] J. L. Sessler, S. J. Weghorn, V. Lynch, M. R. Johnson, *Angew. Chem.* **1994**, *106*, 1572–1575; *Angew. Chem. Int. Ed. Engl.* **1994**, *33*, 1509–1512.
- [19] E. Vogel, M. Bröring, J. Fink, D. Rosen, H. Schmickler, J. Lex, K. W. K. Chan, Y.-D. Wu, D. A. Plattner, M. Nendel, K. N. Houk, *Angew. Chem.* **1995**, *107*, 2705–2709; *Angew. Chem. Int. Ed. Engl.* **1995**, *34*, 2511–2514.
- [20] M. Bröring, J. Jendry, L. Zander, H. Schmickler, J. Lex, Y.-D. Wu, M. Nendel, J. Chen, D. A. Plattner, K. N. Houk, E. Vogel, *Angew. Chem.* **1995**, *107*, 2709–2711; *Angew. Chem. Int. Ed. Engl.* **1995**, *34*, 2515–2517.
- [21] A. Werner, M. Michels, L. Zander, J. Lex, E. Vogel, *Angew. Chem.* **1999**, *111*, 3866–3870; *Angew. Chem. Int. Ed.* **1999**, *38*, 3650–3653.
- [22] J.-Y. Shin, H. Furuta, K. Yoza, S. Igarashi, A. Osuka, *J. Am. Chem. Soc.* **2001**, *123*, 7190–7191.
- [23] N. Sprutta, L. Latos-Grażyński, *Chem. Eur. J.* **2001**, *7*, 5099.
- [24] H. Rath, J. Sankar, H. PrabhuRaja, T. K. Chandrashekar, B. S. Joshi, R. Roy, *Chem. Commun.* **2005**, 3343–3345.
- [25] J. Braun, M. Koecher, M. Schlabach, B. Wehrle, H.-H. Limbach, E. Vogel, *J. Am. Chem. Soc.* **1994**, *116*, 6593–6604.
- [26] C. S. Wannere, K. W. Sattelmeyer, H. F. Schaefer III, P. von R. Schleyer, *Angew. Chem.* **2004**, *116*, 4296–4302; *Angew. Chem. Int. Ed.* **2004**, *43*, 4200–4206. Alternatively, MCSCF calculations could be used; see: C. van Wüllen, W. Kutzelnigg *Chem. Phys. Lett.* **1993**, *205*, 563; W. Kutzelnigg, C. van Wüllen, U. Fleischer, R. Franke, T. v. Mourik, *NATO ASI Ser. Ser. C* **1993**, *386*, 141.
- [27] Alternatively, the change in topology can be demonstrated by counting the number of *trans* bonds (see Ref. [6]) along the [28]annulenoid conjugation pathway. Compound **1-M** has an odd number of *trans* bonds, and **1-H** has an even number of *trans* bonds.
- [28] Crystal data for **1** are given in the Supporting Information. CCDC-635756 contains the supplementary crystallographic data for this paper. These data can be obtained free of charge from The Cambridge Crystallographic Data Centre via [www.ccdc.cam.ac.uk/data\\_request/cif](http://www.ccdc.cam.ac.uk/data_request/cif).